OXFORD

Social preferences correlate with cortical thickness of the orbito-frontal cortex

Andrea Fariña, [iD][1,2] Michael Rojek-Giffin,[1,2] Jörg Gross, [iD][1,2] and Carsten K.W. De Dreu [iD][1,2,3]

[1]Institute for Psychology, Leiden University, Leiden 2300 RB, The Netherlands, [2]Leiden Institute for Brain and Cognition, Leiden University, Leiden 2300 RB, The Netherlands, and [3]Center for Research in Experimental Economics and Political Decision Making, University of Amsterdam, Amsterdam, 1018 WB, The Netherlands

Correspondence should be addressed to Andrea Fariña, Leiden University, PO 9555, Leiden 2300 RB, The Netherlands. E-mail: a.farina@fsw.leidenuniv.nl.

Abstract

Humans differ in their preferences for personal rewards, fairness and others' welfare. Such social preferences predict trust, public goods provision and mutual gains bargaining and have been linked to neural activity in regions involved in reward computation, cognitive control and perspective-taking. Although shaped by culture, social preferences are relatively stable across time, raising the question whether differences in brain anatomy predict social preferences and their key components—concern for personal outcomes and concern for others' outcomes. Here, we examine this possibility by linking social preferences measured with incentivized economic games to 74 cortical parcels in 194 healthy humans. Neither concerns for personal outcomes nor concerns for the outcomes of others in isolation were related to anatomical differences. However, fitting earlier findings, social preferences positively scaled with cortical thickness in the left olfactory sulcus, a structure in the orbital frontal cortex previously shown to be involved in value-based decision-making. Consistent with work showing that heavier usage corresponds to larger brain volume, findings suggest that pro-social preferences relate to cortical thickness in the left olfactory sulcus because of heavier reliance on the orbital frontal cortex during social decision-making.

Key words: brain anatomy; social value orientation; decision-making

Introduction

As group-living animals, many of the decisions humans make not only affect their own outcomes but those of others around them as well. When maximizing personal gains comes at a cost to others, humans need to trade off their preference for personal reward against preferences for fairness and others' welfare (Fehr and Camerer, 2007; Van Dijk and De Dreu, 2021). How individuals make this trade-off defines their social preferences. Humans differ in their concern for fairness and others' welfare, and such differences in social preferences explain decision-making in a variety of situations, including extending and reciprocating trust (Ashraf *et al.*, 2006; Kanagaretnam *et al.*, 2009), providing for public goods (Balliet *et al.*, 2009) and seeking a mutually beneficial outcome in negotiations (De Dreu *et al.*, 2000). Brain imaging studies have linked social preferences to neural activity in the dorsolateral prefrontal cortex associated with monitoring and executive control (Baumgartner *et al.*, 2011), the amygdala and insular cortex associated with the regulation of emotion (Haruno *et al.*, 2014; Liu *et al.*, 2019) and the temporoparietal junction associated with empathy and perspective-taking (namely, Theory of Mind; Emonds *et al.*, 2014; for recent reviews, see De Dreu, Gross, Fariña & Ma, 2020; Hung *et al.*, 2020; Amodio and Cikara, 2021).

Being pivotal to living and working in groups, social preferences are shaped by culture and socialization on the one hand (Van Lange, 1999) and evolutionary selection pressures on the other (Darwin, 1859; Bowles, 2009). Akin to personality traits, social preferences are relatively stable across time and operate in addition to situational pressures (Van Lange, 1999; Murphy and Ackerman, 2014; De Dreu and Gross, 2019). Personality traits related to social preferences, such as agreeableness, have been shown to be related to differences in brain anatomy (Riccelli *et al.*, 2017). Along similar lines, Churchwell and Yurgelun-Todd (2013) found a positive relationship between insula thickness and impulsivity, while Muhlert and Lawrence (2015) identified that rash impulsivity correlated with lower volume of the ventral striatum.

Here, we examine the possibility that social preferences are likewise associated with differences in brain structure and anatomy. Indeed, previous research has shown that cortical thickness of the dorsolateral prefrontal cortex predicts strategic choices in economic games (Yamagishi *et al.*, 2016) and that gray matter volume in the right temporoparietal junction varies with individual differences in altruistic giving (Morishima *et al.*, 2012). Currently lacking, however, is a statistically powerful and comprehensive whole-brain analysis on the relationship between general social preferences and anatomical differences. Here we fill this gap. We measured social preferences using a standardized and incentivized decision task in a large sample of healthy male and female volunteers. Earlier work using this task showed that social preferences reliably predict HEXACO Honesty-Humility and Big Five Agreeableness scores, cooperation in economic games, as well as charitable donations and involvement in volunteering (Pletzer *et al.*, 2018; Van Dijk and De Dreu, 2021). We investigate how pro-social preferences, and the underlying concern for personal rewards and concern for others' rewards, relate to cortical thickness of 74 distinct bilateral brain areas with identifiable functionalities for human cognition and behavior. Figure 1 shows a graphical display of these anatomical structures for the left hemisphere.

To guide our analyses, we reviewed findings from functional neuroimaging studies linking brain regions to social decision-making. Social decision-making has been argued to rely on the capacity to form expectations of others' cooperative behavior (Declerck and Bogaert, 2008; Emonds *et al.*, 2011), on the cognitive control of both selfish and pro-social impulses (Baumgartner *et al.*, 2011; Rand *et al.*, 2013) and on the ability to perform broad utility-based calculations (Fehr and Schmidt, 2006). Table 1 shows, for each anatomical parcel in Figure 1, its mapping on functional regions and neural networks. We identified three (partly overlapping and interacting) neural networks with well-documented functionalities for social preferences and concern for self and others in particular: the Cognitive Control Network that includes the dorsolateral prefrontal cortex, the anterior cingulate and the orbitofrontal cortex (OFC) (Duncan and Owen, 2000; Aron, Robins, & Poldrack, 2004); the Default Mode Network that includes the (ventro)medial prefrontal cortex, the posterior cingulate cortex (precuneus), the temporoparietal junction and the anterior temporal pole and cortex (Buckner *et al.*, 2008; Blakemore, 2008; Bressler and Menon, 2010; Wittmann *et al.*, 2018); and the Theory of Mind Network that includes the medial prefrontal cortex, the superior temporal sulcus, the precuneus, the temporoparietal junction, the anterior cingulate cortex and the inferior frontal gyrus (Gallagher and Frith, 2003; Spreng *et al.*, 2009; Decety, 2010; Schurz *et al.*, 2014). Whether and to what extent anatomical features of these or other parcels are associated with social preferences remain largely unknown and are examined here in terms of cortical thickness.
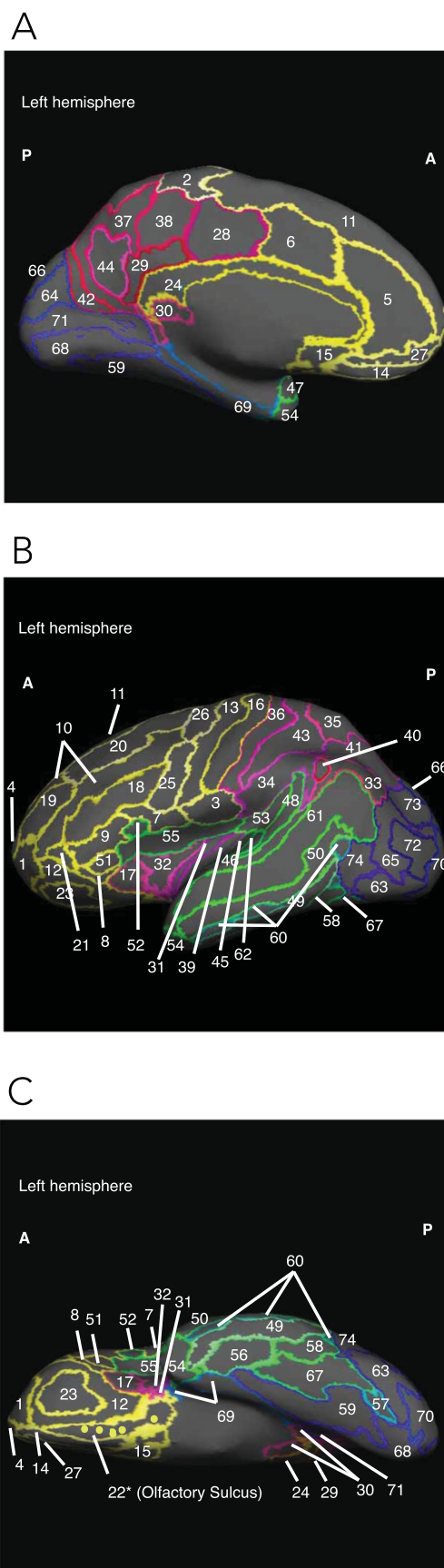

Fig. 1. Brain regions by lobe. (A) Medial view of the left hemisphere; (B) lateral view of the left hemisphere; (C) inferior view of the left hemisphere. Yellow hues indicate frontal regions, green indicates the temporal lobe, pink is parietal and blue is occipital. Numbers indicate different parcels.

Table 1. Anatomical parcels by lobe according to the Destrieux Atlas (ID, see Figure 1), with associated functional regions and neural networks involved in empathy, (cognitive) control and reward processing

ID	Anatomical parcel	Functional regions (networks)	Empathy	(Cognitive) control	Reward processing
Frontal lobe					
1	Frontomarginal gyrus and sulcus	VMPFC; OFC (DMN; ToM)	Moll et al. (2002); Lewis et al. (2011)	Koechlin and Hyafil (2007)	Hare et al. (2009); Levy and Glimcher (2012)
2	Paracentral gyrus and sulcus	SMA	Fan et al. (2011)	–	–
3	Subcentral gyrus and sulcus	SMA	Adolphs et al. (2000); Molenberghs et al. (2012)	–	–
4	Transverse frontopolar gyri	VMPFC; OFC (CNN, DMN; ToM)	Shamay-Tsoory et al. (2009); Lewis et al. (2011)	Koechlin and Hyafil (2007); Boorman et al. (2009)	Hare et al. (2009); Levy and Glimcher (2012)
5	Anterior cingulate gyrus and sulcus	ToM	Van Overwalle and Baetens (2009); Schurz et al. (2014)	Botvinick et al. (2001); Kerns et al. (2004)	Kennerley et al. (2006)
6	Mid anterior cingulate gyrus and sulcus	ToM	Lamm et al. (2011)	Shackman et al. (2011)	Kennerley et al. (2006)
7	Pars opercularis	IFG (ToM)	Schurz et al. (2014)	Derrfuss et al. (2005)	–
8	Pars orbitalis	IFG (ToM)	Schurz et al. (2014)	Derrfuss et al. (2005)	–
9	Pars triangularis	IFG (ToM)	Schurz et al. (2014)	Derrfuss et al. (2005)	–
10	Middle frontal gyrus	DLPFC (CCN)	–	Buchsbaum et al. (2005); Hare et al. (2009)	–
11	Superior frontal gyrus	SMA	Farrow et al. (2001); Fan et al. (2011)	Bonini et al. (2014)	–
12	Orbital gyri	OFC (CCN; ToM)	Abu-Akel and Shamay-Tsoory (2011)	–	Levy and Glimcher (2012)
13	Precentral gyrus	M1	–	–	–
14	Rectus gyrus	OFC (CCN; ToM)	Abu-Akel and Shamay-Tsoory (2011)	–	Levy and Glimcher (2012)
15	Subcallosal gyrus		–	–	–
16	Central sulcus	M1 and S1 (ToM)	–	–	–
17	Anterior circular sulcus		Lamm et al. (2011)	McKenna et al. (2017)	Liu et al. (2011)
18	Inferior frontal sulcus	OFC (CCN; ToM)	Carrington and Bailey (2009)	Derrfuss et al. (2005); Pan et al. (2018)	Levy and Glimcher (2012)
19	Middle frontal sulcus		–	Buchsbaum et al. (2005); Hare et al. (2009)	–
20	Superior frontal sulcus	SMA	Fan et al. (2011)	Bonini et al. (2014)	–
21	Lateral orbital sulcus	OFC; VMPFC (CNN, DMN, ToM)	Moll et al. (2002); Lewis et al. (2011)	–	Hare et al. (2009); Levy and Glimcher (2012)
22	Olfactory sulcus	OFC (CCN, ToM)	Moll et al. (2002); Lewis et al. (2011)	–	Hare et al. (2009); Levy and Glimcher (2012)
23	H-shaped sulcus	OFC (CCN, ToM)	Moll et al. (2002); Lewis et al. (2011)	–	Hare et al. (2009); Levy and Glimcher (2012)
24	Pericallosal sulcus		–	–	–
25	Inferior precentral sulcus	SMA	Fan et al. (2011)	–	–
26	Superior precentral sulcus	SMA	Fan et al. (2011)	–	–
27	Suborbital sulcus	OFC (CCN, ToM)	Moll et al. (2002); Lewis et al. (2011)	–	Hare et al. (2009); Levy and Glimcher (2012)
Parietal lobe					
28	Mid posterior cingulate gyrus and sulcus	DMN	Schlaffke et al. (2015)	Kragel et al. (2018)	–
29	Dorsal posterior cingulate gyrus	DMN	Schlaffke et al. (2015)	Kragel et al. (2018)	–
30	Ventral posterior cingulate gyrus	DMN	Schlaffke et al. (2015)	Kragel et al. (2018)	–
31	Long insular gyri and central insular sulcus		–	–	–
32	Short insular gyrus		Fan et al. (2011)	–	–
33	Angular gyrus	TPJ (DMN, ToM)	Schurz et al. (2017)	Cabeza et al. (2012)	–
34	Supramarginal gyrus	TPJ (DMN, ToM)	Schurz et al. (2017)	Cabeza et al. (2012)	–

(continued)

Table 1. (Continued)

ID	Anatomical parcel	Functional regions (networks)	Empathy	(Cognitive) control	Reward processing
35	Superior parietal gyrus		–	McKenna *et al.* (2017)	–
36	Postcentral gyrus		Fan *et al.* (2011)	–	–
37	Precuneus		Schurz *et al.* (2014)	–	–
38	Marginal sulcus		–	–	–
39	Inferior circular sulcus		–	–	–
40	Jensen sulcus	TPJ (DMN, ToM)	Schurz *et al.* (2017)	Cabeza *et al.* (2012)	–
41	Intraparietal sulcus	TPJ (DMN, ToM)	Schurz *et al.* (2017)	McKenna *et al.* (2017)	–
42	Parieto occipital sulcus		–	–	–
43	Postcentral sulcus	S1 (ToM)	–	–	–
44	Subparietal sulcus		–	–	–
	Temporal lobe				
45	Anterior transverse temporal gyri	AC (DMN)	–	–	–
46	Lateral superior temporal gyrus		Zahn *et al.* (2007)	–	–
47	Planum polare	AC	–	–	–
48	Planum temporale	AC	–	–	–
49	Inferior temporal gyrus		–	–	–
50	Middle temporal gyrus		Carrington and Bailey (2009)	–	–
51	Horizontal lateral fissure	S2	–	–	–
52	Vertical lateral fissure	S2	–	–	–
53	Posterior lateral fissure	S2	–	–	–
54	Temporal pole	DMN	Carrington and Bailey (2009)	McKenna *et al.* (2017)	–
55	Superior circular sulcus		–	–	–
56	Anterior collateral sulcus		–	–	–
57	Posterior collateral sulcus		–	–	–
58	Lateral occipital-temporal sulcus		–	–	–
59	Medial occipito-temporal and lingual sulci		–	–	–
60	Inferior temporal sulcus		–	–	–
61	Superior temporal sulcus		Molenberghs *et al.* (2016); Isik *et al.* (2017)	–	–
62	Transverse temp. sulcus	AC	–	–	–
	Occipital lobe				
63	Inferior occ. gyrus and sulcus		–	–	–
64	Cuneus	V1	–	–	–
65	Middle occipital gyrus		Carrington and Bailey (2009)	–	–
66	Superior occipital gyrus		Carrington and Bailey (2009)	–	–
67	Fusiform gyrus		Carrington and Bailey (2009)	–	–
68	Lingual gyrus		Carrington and Bailey (2009)	Buchsbaum *et al.* (2005)	–
69	Parahippocampal gyrus		–	–	–
70	Occipital pole		–	–	–
71	Calcarine sulcus	V1	–	–	–
72	Lunatus sulcus	V1, V2	–	–	–
73	Superior and transversal occipital sulci		–	–	–
74	Anterior occipital sulcus		Carrington and Bailey (2009)	–	–

Notes: VMPFC = ventromedial prefrontal cortex; OFC = orbitofrontal cortex; IFG = inferior frontal gyrus; DLPFC = dorsolateral prefrontal cortex; M1 = motor cortex (primary); S1 = somatosensory cortex (primary); S2 = somatosensory cortex (secondary); V1 = visual cortex (primary); V2 = visual cortex (secondary); AC = auditory cortex; TPJ = temporoparietal junction; CCN = cognitive control network; DMN = default mode network; SMA = supplementary motor area.

Materials and methods

Participants and ethics

To acquire social preferences and structural brain images, 214 participants were tested individually and compensated 50 euros in addition to their earnings from decision-making (subjects were paid out one randomly drawn decision, on average earning €5). Sample size was based on earlier work on social value orientation (SVO) and cooperative decision-making in experimental games, typically showing that 40% of research samples can be classified as pro-social and another 40% as selfish (e.g. Van Lange, 1999). Our sample size fell in the upper range of earlier studies examining correlations between personality dimensions and brain anatomy (i.e. ranging between $50 < N < 500$; see, e.g., Fischl and Dale, 2000; Haas *et al.*, 2015; Kitayama *et al.*, 2017; Morishima *et al.*, 2012; Riccelli *et al.*, 2017; Yamagishi *et al.,* 2016). The experimental protocol received approval from the Ethics Review Board of the University of Amsterdam (ethics approval number 2015-EXT-4366). Participants provided written informed consent and received a full debriefing. The experiments involved no deception and decisions were fully incentivized.

Brain imaging

All brain images were acquired using a Philips Achieva 3T MRI scanner and a 32-channel SENSE head coil at the University of Amsterdam. A survey scan was made for spatial planning of the subsequent scans. Following the survey scan, a 3-min structural T1-weighted scan was acquired using three-dimensional fast-field echo (repetition time = 82 ms, echo time = 38 ms, flip angle = 8, field-of-view = 240 × 188 mm, 220 slices acquired using single-shot ascending slice order and a voxel size of 1 × 1 × 1 mm). Cortical reconstruction and segmentation were performed with the Freesurfer image analysis suite (http://surfer.nmr.mgh.harvard.edu/). This processing included removal of non-brain tissue, automated Talairach transformation, segmentation of the subcortical white matter and deep gray matter volumetric structures, intensity normalization, tessellation of the gray matter white matter boundary and automated topology correction. Once the cortical models were complete, they were aligned to a spherical atlas which is based on individual cortical folding patterns to match cortical geometry across subjects (Fischl *et al.*, 1999), and the cerebral cortex was parcellated into 74 parcels on each hemisphere with respect to gyral and sulcal structures (Destrieux *et al.*, 2010). Cortical thickness was calculated as the closest distance from the gray/white boundary to the gray/CSF boundary at each vertex on the tessellated surface (Fischl and Dale, 2000). These outputs were then visually inspected to ensure the quality of the images and their segmentation.

Social preferences

Either before or after brain imaging, we assessed social preferences using the SVO Ring Measure (Liebrand, 1984; Liebrand and McClintock, 1988; Van Lange, 1999). The Ring Measure has strong convergent validity with related measures of social preferences, acceptable test–retest reliability with time gaps up to 2 months (Murphy and Ackerman, 2014), and predicts trust and trustworthiness (Kanagaretnam *et al.*, 2009), public good provision (Liebrand, 1984; Pletzer *et al.*, 2018), and fairness and conciliatory behavior in bargaining (De Dreu and Van Lange,

1995). Thus, SVO measures a person's chronic tendency to cooperate with others, as opposed to more transient measures of other-regarding preferences that may change conditional on who they are interacting with and the intentions of those they are interacting with (Fehr and Schmidt, 2006; Van Dijk and De Dreu, 2021).

The Ring Measure requires subjects to make 24 incentivized choices between pairs of own-other monetary outcomes, forcing participants to systematically trade their own economic welfare with the welfare of another person (Supplementary Table S1). Each pair represents an outcome on a circle with radius €15 and origin €15 for the self and €15 for an anonymous other (Supplementary Figure S1). Each choice involves two adjacent pairs on the circle. For instance, one question confronts participants with a choice between €28 for him/herself and €22.50 for an anonymous partner (the other) or €29.50 for the self and €18.90 for the other. The latter option increases the payoff for the participant at the expense of the other person, while the first option is more pro-social and increases the payoff of the other person at the expense of the payoff for oneself.

To obtain a measure of a participant's SVO, the average amount allotted to the self is divided by the average amount allotted to the other. This ratio is then converted into an angle measurement, by taking its inverse tangent. Traditionally, the angle is used to classify subjects into distinct SVO categories (Figure 2; Supplementary Table S1 and Figure S1). Here we used the angle as a continuous measure of pro-sociality and transformed participants' degree measures such that an angle measurement of 0° corresponds to a decision pattern that sacrifices own payoff to hurt the other person (traditionally labeled 'sadistic', a pattern that is very uncommon and that none of our subjects exhibited). Through this transformation, we achieved a positive correlation between the degree of the SVO angle and the participant's willingness to trade money for self in return for money for the other person.

Next to its angle, for each participant, the SVO measure allows to calculate a vector length reflecting the consistency in allocation choices: the shorter the vector, the more inconsistent the participant (Murphy and Ackerman, 2014). A perfectly consistent participant has a vector length of 1.25. Twenty participants had a vector length shorter than 0.625 (50% of this maximum vector), indicating non-consistent random behavior across trials. This prohibits reliable inference of social preferences. We excluded these 20 participants from the main analyses, leaving a total sample of $N = 194$ with complete data (mean age = 24.15, s.d. = 1.90, 105 females). Including these 20 participants reduced effect sizes but nevertheless permitted the same conclusions. For six participants, age and gender data were missing and replaced by the average age and randomly assigned gender (omitting these subjects from the main analyses resulted in descriptively and statistically similar results). Neither gender nor age were significantly correlated with SVO angle ($SVO_{male} = 137.40$, SE = 0.34; $SVO_{female} = 137.35$, SE = 0.23; $b = -0.05$, $P = 0.98$; r(age, SVO) = −0.092, $P = 0.20$).

The SVO angle is a composite of each participant's weight to self (W_{self}) and weight to other (W_{other}). W_{self} is defined as the difference of money allocated to oneself and the median amount of total money to be gained for the self (€360), divided by the maximal difference between the self and the other's outcomes (€60). This normalizes the result such that a median score corresponds to a value of zero. Accordingly, a subject who allocates the maximum (minimum) amount of money to oneself will have a score of 0.5 (−0.5) for W_{self}. Similarly, W_{other} is defined as the difference of money allocated to the other and the median
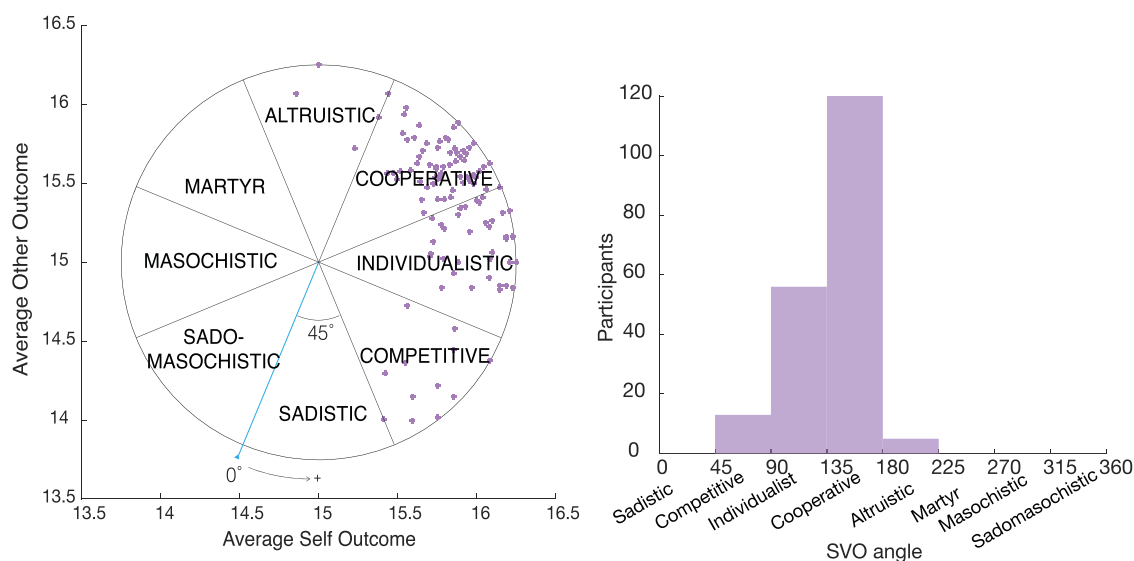
Fig. 2. Social value orientation (SVO) categories by degree. Left: each cross represents one participant. A SVO degree of 0 corresponds to a perfectly sadistic orientation (sacrificing own outcome to reduce the outcome of the other person). As SVO degree increases, so does a person's willingness to trade money for the self in return for money for the other. Right: histogram of participants by SVO category.

amount of total money to be gained for the other (€360), divided by the maximal difference between the self and the other's outcomes (€60). A subject who allocates the maximum (minimum) amount of money to the other will have a score of 0.5 (−0.5) for W_{other}. These weights are in line with the underlying psychological motivations for the categories shown in Figure 2 (e.g. if a person falls within the 'competitive' category, it is inferred that she/he tries to maximize the positive difference between the payoff for oneself and the payoff for the other) and described in Murphy and Ackerman (2014; Supplementary Table S1). To illustrate, if a participant answered all 24 Ring Measure questions in such a way that they allocated €380.40 to themselves and €370.90 to the other, they would have a $W_{self} = (380.40 − 360)/60 = 0.34$ and a $W_{other} = (370.90 − 360)/60 = 0.18$.

Data analytic strategy

To examine the relationship between SVO and cortical thickness, we categorized each of the cortical parcels into the four brain lobes: the frontal (27 parcels), temporal (18 parcels), parietal (17 parcels) and occipital (12 parcels) (Destrieux *et al.*, 2010; see Figure 1). The insular and the cingulate gyri and sulci (parcels numbered 5, 6, 17, 28, 29, 31, 32, 39 and 55 in Figure 1) were classified into one of these four lobes based on proximity. For each cortical parcel, we performed regressions of the type:

$$\text{Cortical thickness(parcel)} = C + \beta_1(\text{SVO}) + \beta_2(\text{age}) + \beta_3(\text{gender})$$
$$+ \beta_4(\text{average thickness}) \quad (1)$$

where β_1 is the standardized regression weight for SVO, β_2 and β_3 the standardized weights for age and gender, respectively, β_4 the regression weight for average thickness of the corresponding left or right hemisphere and ε estimates the error variance.

To identify whether the relationship between cortical thickness and SVO varies by hemisphere, as others have found (Morishima *et al.*, 2012; Yamagishi *et al.*, 2016), regressions were computed separately for left and right hemispheres, with the

average thickness of the corresponding hemisphere included as a control variable. Table A1 (Appendix) lists the observed regression weights for each parcel. Crucially, the number of tests performed increases the risk of false-positives. We maintained this risk at a Type I error at 5% through the Freedman and Lane (1983) permutation testing procedure. Permutation tests estimate statistical significance directly from the data being used, and the estimated familywise error rate has been shown to be more reliable than when using parametric methods (Winkler *et al.*, 2014; Eklund *et al.*, 2016). Thus, to test whether β_1 was different from zero, we first computed a null distribution of β_1 by permuting the real data while keeping the relationship between each participant's cortical thickness and the control variables unchanged. We then used this null distribution to find the 5% threshold at which to compare our original t-statistics for β_1. Specifically, for each of the four lobes, we (i) obtained t-statistics for the regression coefficient β_1 for each cortical parcel; (ii) ran reduced regression models without the variable of interest (SVO) and saved the fitted values of cortical thickness as well as the residuals from this model; (iii) permuted the residuals from the reduced model to create a permuted fitted value of cortical thickness and (iv) estimated the full regression model using the permuted fitted values from (iii) as the dependent variable:

$$\text{Permuted cortical thickness(parcel)} = C + \beta_1(\text{SVO}) + \beta_2(\text{age})$$
$$+ \beta_3(\text{gender})$$
$$+ \beta_4(\text{average thickness}) \quad (2)$$

We saved the maximum t-statistic of all parcels within each lobe; (v) repeated steps (iii) and (iv) 5000 times; (vi) compared the original t-statistics from equation (1) to the distribution of 5000 maximum t-statistics of step (v) to obtain a corrected P-value for the regression coefficient of SVO. This procedure is equivalent to testing H0 that $\beta_1 = 0$. Permutation results are shown in Table A1 (Appendix).
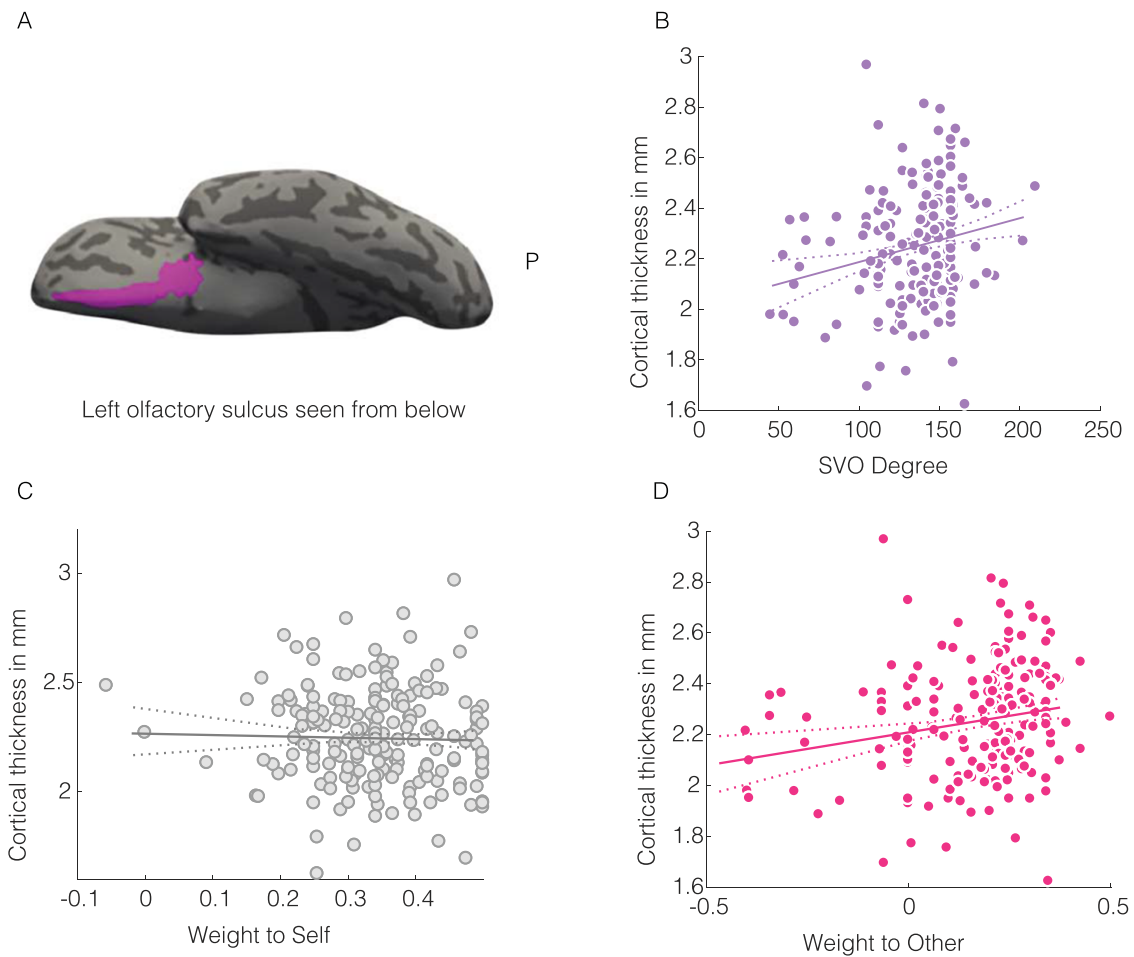
Fig. 3. Cortical thickness of the left olfactory sulcus (OS) relates to social preferences. (A) View of left OS from below on an inflated surface. (B) SVO degree—OS pairs with best fitting linear regression, controlling for age, gender, and average thickness of the left hemisphere. (C) Cortical thickness of the left olfactory sulcus and weight to self. Solid line represents the regression coefficient of weight to self after controlling for age, gender, weight to other, and average thickness of the left hemisphere. (D) Cortical thickness of the left olfactory sulcus and weight to other. Solid line represents the regression coefficient of weight to other after controlling for age, gender, weight to self and average thickness of the left hemisphere. Dashed lines represent the 95% confidence interval. Dots represent individual participants.

Results

Fitting previous research, we found no significant relationship between cortical thickness and SVO angle within the occipital lobe (Table A1, Appendix). Importantly, we also found no significant relations between SVO angle and regions in the temporal and parietal lobes after permutation testing - regions that earlier work associated with empathy or theory of mind (see Table A1, Appendix). At the same time, however, we did observe a robust positive relationship between SVO angle and the cortical thickness of the olfactory sulcus—an area of the OFC which is functionally involved in value-based decision-making (Table 1, Figure 3A). Stronger pro-social preferences linearly scaled with the cortical thickness of the olfactory sulcus (Figure 3B; $\beta = 0.0017$, permuted $P = 0.03$).

The SVO angle is a composite of two variables—concern for self (W_{self}) and concern for other (W_{other})—that are only partially correlated within the SVO measure and may have independent (and perhaps even opposite) relations to neural regions, both functionally and structurally. Accordingly, we repeated our regression analyses substituting SVO angle by W_{self} and W_{other},

using the permutation testing procedures described above for $\beta \times SVO$ but now with $\beta \times W_{self}$ and $\beta \times W_{other}$ as the variables of interest:

$$\text{Cortical thickness(parcel)} = C + \beta_5(W_{self}) + \beta_6(W_{other})$$
$$+ \beta_3(\text{gender})$$
$$+ \beta_4(\text{average thickness}) \quad (3)$$

After correcting for multiple comparisons using permutation testing, we found null results for the occipital, temporal, parietal lobes and W_{self} or W_{other} (Table A1, Appendix). Further qualifying results for SVO angle, we found a positive relationship between the cortical thickness of the left olfactory sulcus and W_{other} (Figure 3D; $\beta = 0.26$, permuted $P = 0.06$) and no such relationship with W_{self} (Figure 3C; $\beta = -0.08$, permuted $P = 1$). This suggests that the relationship between SVO angle and cortical thickness of the left olfactory sulcus resides in differences in the weight given to other's outcomes and not in the weight given to own outcomes.

Conclusions and discussion

Previous structural (Sul, et al., 2015; Nash *et al.*, 2015; Yamagishi *et al.*, 2016; Sul, Guöroğlu, Crone, & Chang, 2017) and functional imaging studies (Baumgartner *et al.*, 2011; Emonds *et al.*, 2011; Balconi and Canavesio, 2014; Christov-Moore *et al.*, 2017) on cognitive control and value-based decision-making gave us reason to expect a relationship between cortical thickness in the dorsolateral prefrontal cortex (Areas 10, 19 in Figure 1A) and social preferences. Our comprehensive whole-brain analyses did not, however, reveal such linkages. Likewise, results did not show any relationship between social preferences and cortical thickness of areas in the parietal lobe that earlier work associated with Theory of Mind (i.e. the temporoparietal junction; see Saxe and Kanwisher, 2003; Van Overwalle, 2009; Molenberghs *et al.*, 2016).

These negative results aside, our comprehensive whole-brain analysis revealed a significant correlation between SVO angle and cortical thickness of the OFC (Areas 4, 12, 14, 18, 21, 22, 23 in Figures 1A and 1B). The OFC, a critical region for value-based decision-making (Rolls and Grabenhorst, 2008), has been previously linked to decisions involving social preferences (Fehr and Camerer, 2007). Kitayama and colleagues (2017) recently showed that OFC cortical volume inversely predicted interdependent self-construal—the view of the self in relation to others, while Haas and colleagues (2015) found that self-reported trust scores were positively associated with gray matter volume in the bilateral ventromedial prefrontal cortex.

Our results are in line with these findings and show that stronger prosocial preferences associate with the thickness of the left olfactory sulcus (Area 22 in Figure 1C). One possible explanation for the link between SVO angle and the OFC is that prosocial individuals take not only their own outcome into account but also those of others, rendering their decision-making process computationally more demanding than that of pro-self individuals. Indeed, previous research on SVO has shown that cooperators and competitors have, compared to individualists, longer response latencies (Liebrand and McClintock, 1988; Chen and Fischbacher, 2016) and engage in greater information search (Fiedler *et al.*, 2013) when making allocation decisions. Possibly, these more complex value computations may require greater involvement from the OFC. In line with this reasoning, research has found that sensorimotor experience leads to structural brain changes in human (Maguire *et al.*, 2000; Draganski *et al.*, 2004) and macaque (Quallo *et al.*, 2009) gray matter, especially in sensorimotor areas.[1] Furthermore, there is some evidence that social complexity, including social network size, correlates with the size of prefrontal regions in various species, including the macaque (Sallet *et al.*, 2011; Wittmann *et al.*, 2018; also see Bickart *et al.*, 2011) and cleaner fish (Triki *et al.*, 2019). However, since the directionality of social behavior and brain anatomy is not yet fully understood, it may be the case that existing brain structure leads more readily to certain behaviors, rather than the other way around. Combined,

these works suggest that extensive engagement of a particular brain region correlates with its cortical thickness, and this may explain the observed correlations between cortical thickness of the left olfactory sulcus and pro-social preferences reported here.

Our analyses covered the whole brain in a relatively large sample of healthy participants. Whereas significant correlations were found between the cortical thickness of particular brain regions and our measure of social preferences (see Table A1, Appendix), these findings did not survive rigorous permutation testing. Even in the one case that did survive permutation testing—the cortical thickness of the left olfactory sulcus—the amount of variance explained by social preferences is rather small. In other words, differences in brain anatomy contribute little to the direct prediction of individual differences in social preferences (also see note 1). However, in using a standard parcellation map, some of the larger parcels might mask variations in functionality within these parcels. A more meticulous parcellation of such areas could reveal additional relationships between cortical thickness and social preferences that were not identified here. Future work could investigate more fine-grained parcellations of different brain areas.

While people chronically differ in their social preferences, pro-social behavior often depends on and changes as a function of the environment or the history of social interactions. Such situation dependence is highly adaptive, since unconditional pro-sociality can be easily exploited and this may explain why we found no strong relations to brain anatomy. Yet pro-sociality also renders decision-making more complex. Decision-makers have to incorporate the welfare of others' in their decision-making, and this computational complexity may manifest in brain anatomy, in particular that of the OFC.

Conflict of interest

The authors declare that the research was conducted in the absence of any commercial or financial relationships that could be construed as a potential conflict of interest.

Supplementary data

Supplementary data are available at SCAN online.

Data availability statement

As the data for this study were collected in collaboration with several research groups, raw data sharing must be coordinated between co-owners and is available upon request. Derived data supporting the findings of this study will be openly available.

[1] Previous studies have shown some correlations between social values and gray matter volume in subcortical structures, including the amygdala (Bickart *et al.*, 2011). We explored neuroanatomical variability in subcortical nuclei by regressions social value orientation (angle, W_{self} and W_{other}) on the gray matter volume of the amygdala, the caudate, the pallidum, putamen and accumbens, while controlling for age, gender and intracranial volume. Even without correcting for multiple comparisons, we found, however, no significant differences. The corresponding author can be contacted for further detail.

References

Abu-Akel, A., Shamay-Tsoory, S. (2011). Neuroanatomical and neurochemical bases of theory of mind. *Neuropsychologia*, **49**(11), 2971–84.

Adolphs, R., Damasio, H., Tranel, D., Cooper, G., Damasio, A.R. (2000). A role for somatosensory cortices in the visual recognition of emotion as revealed by three-dimensional lesion mapping. *Journal of Neuroscience*, **20**(7), 2683–90.

Amodio, D., Cikara, M. (2021). The social neuroscience of prejudice. *Annual Review of Psychology*, **2021**(72), 439–69.

Aron, A.R., Robbins, T.W., Poldrack, R.A. (2004). Inhibition and the right inferior frontal cortex. *Trends in Cognitive Sciences*, **8**(4), 170–7.

Ashraf, N., Bohnet, I., Piankov, N. (2006). Decomposing trust and trustworthiness. *Experimental Economics*, **9**(3), 193–208.

Balconi, M., Canavesio, Y. (2014). High-frequency rTMS on DLPFC increases prosocial attitude in case of decision to support people. *Social Neuroscience*, **9**(1), 82–93.

Balliet, D., Parks, C., Joireman, J. (2009). Social value orientation and cooperation in social dilemmas: a meta-analysis. *Group Processes & Intergroup Relations*, **12**(4), 533–47.

Baumgartner, T., Knoch, D., Hotz, P., Eisenegger, C., Fehr, E. (2011). Dorsolateral and ventromedial prefrontal cortex orchestrate normative choice. *Nature Neuroscience*, **14**(11), 1468–74.

Bickart, K.C., Wright, C.I., Dautoff, R.J., Dickerson, B.C., Barrett, L.F. (2011). Amygdala volume and social network size in humans. *Nature Neuroscience*, **14**(2), 163–4.

Blakemore, S.J. (2008). The social brain in adolescence. *Nature Reviews Neuroscience*, **9**(4), 267–77.

Bonini, F., Burle, B., Liégeois-Chauvel, C., Régis, J., Chauvel, P., Vidal, F. (2014). Action monitoring and medial frontal cortex: leading role of supplementary motor area. *Science*, **343**(6173), 888–91.

Boorman, E.D., Behrens, T.E., Woolrich, M.W., Rushworth, M.F. (2009). How green is the grass on the other side? Frontopolar cortex and the evidence in favor of alternative courses of action. *Neuron*, **33**(6), 733–43.

Botvinick, M.M., Braver, T.S., Barch, D.M., Carter, C.S., Cohen, J.D. (2001). Conflict monitoring and cognitive control. *Psychological Review*, **108**(3), 624–52.

Bowles, S. (2009). Did warfare among ancestral hunter-gatherers affect the evolution of human social behaviors? *Science*, **324**(5932), 1293–8.

Bressler, S.L., Menon, V. (2010). Large-scale brain networks in cognition: emerging methods and principles. *Trends in Cognitive Sciences*, **14**(6), 277–90.

Buchsbaum, B.R., Greer, S., Wei-Li, C., Berman, K.F. (2005). Meta-analysis of neuroimaging studies of the Wisconsin card-sorting task and component processes. *Human Brain Mapping*, **25**(1), 35–45.

Buckner, R.L., Andrews-Hanna, J.R., Schacter, D.L. (2008). The brain's default network: Anatomy, function, and relevance to disease. In: A. Kingstone, M. B. Miller, editors. *The year in cognitive neuroscience*, 1–38.

Cabeza, R., Ciaramelli, E., Moscovitch, M. (2012). Cognitive contributions of the ventral parietal cortex: an integrative theoretical account. *Trends in Cognitive Sciences*, **16**(6), 338–52.

Carrington, S.J., Bailey, A.J. (2009). Are there theory of mind regions in the brain? A review of the neuroimaging literature. *Human Brain Mapping*, **30**(8), 2313–35.

Chen, F., Fischbacher, U. (2016). Response time and click position: cheap indicators of preferences. *Journal of the Economic Science Association*, **2**(2), 109–26.

Christov-Moore, L., Sugiyama, T., Grigaityte, K., Iacoboni, M. (2017). Increasing generosity by disrupting prefrontal cortex. *Social Neuroscience*, **12**(2), 174–81.

Churchwell, J.C., Yurgelun-Todd, D.A. (2013). Age-related changes in insula cortical thickness and impulsivity: significance for emotional development and decision-making. *Developmental Cognitive Neuroscience*, **6**, 80–6.

Darwin, C. (1859). *On the Origin of Species*. London: John Murray.

De Dreu, C.K.W., Weingart, L.R., Kwon, S. (2000). Influence of social motives on integrative negotiation: a meta-analytic review and test of two theories. *Journal of Personality and Social Psychology*, **78**(5), 889–905.

De Dreu, C.K.W., Gross, J., Fariña, A., Ma, Y. (2020). Group cooperation, carrying-capacity stress, and intergroup conflict. *Trends in Cognitive Sciences*, **24**, 760–76.

De Dreu, C.K.W., Gross, J. (2019). Homo Oeconomicus with a Personality—Trait-based Differences in Decision Making. In A. Schram, A. Ule, editors, *Handbook of Research Methods and Applications in Experimental Economics*. Cheltenham, UK: Edward Elgar. 214–33.

De Dreu, C.K., Van Lange, P.A. (1995). The impact of social value orientations on negotiator cognition and behavior. *Personality & Social Psychology Bulletin*, **21**(11), 1178–88.

Decety, J. (2010). The neurodevelopment of empathy in humans. *Developmental Neuroscience*, **32**(4), 257–67.

Declerck, C.H., Bogaert, S. (2008). Social value orientation: related to empathy and the ability to read the mind in the eyes. *The Journal of Social Psychology*, **148**(6), 711–26.

Derrfuss, J., Brass, M., Neumann, J., Von Cramon, D.Y. (2005). Involvement of the inferior frontal junction in cognitive control: meta-analyses of switching and Stroop studies. *Human Brain Mapping*, **25**(1), 22–34.

Destrieux, C., Fischl, B., Halgren, E. (2010). Automatic parcellation of human cortical gyri and sulci using standard anatomical nomenclature. *NeuroImage*, **53**(1), 1–15.

Draganski, B., Gaser, C., Busch, V., Schuierer, G., Bogdahn, U., May, A. (2004). Changes in grey matter induced by training. *Nature*, **427**(6972), 311–2.

Duncan, J., Owen, A.M. (2000). Common regions of the human frontal lobe recruited by diverse cognitive demands. *Trends in Neurosciences*, **23**(10), 475–83.

Eklund, A., Nichols, T.E., Knutsson, H. (2016). Cluster failure: why fMRI inferences for spatial extent have inflated false-positive rates. *Proceedings of the National Academy of Sciences of the United States of America*, **113**(28), 7900–5.

Emonds, G., Declerck, C.H., Boone, C., Vandervliet, E.J., Parizel, P.M. (2011). Comparing the neural basis of decision making in social dilemmas of people with different social value orientations, a fMRI study. *Journal of Neuroscience, Psychology, and Economics*, **4**(1), 11–24.

Emonds, G., Declerck, C.H., Boone, C., Seurinck, R., Achten, R. (2014). Establishing cooperation in a mixed-motive social dilemma. An fMRI study investigating the role of social value orientation and dispositional trust. *Social Neuroscience*, **9**(1), 10–22.

Fan, Y., Duncan, N.W., De Greck, M., Northoff, G. (2011). Is there a core neural network in empathy? An fMRI based quantitative meta-analysis. *Neuroscience and Biobehavioral Reviews*, **35**(3), 903–11.

Farrow, T.F., Zheng, Y., Wilkinson, I.D., *et al*. (2001). Investigating the functional anatomy of empathy and forgiveness. *Neuroreport*, **12**(11), 2433–8.

Fehr, E., Camerer, C.F. (2007). Social neuroeconomics: the neural circuitry of social preferences. *Trends in Cognitive Sciences*, **11**(10), 419–27.

Fehr, E., Schmidt, K.M. (2006). The economics of fairness, reciprocity and altruism–experimental evidence and new theories. In: Kolm, S.C., Ythier, J.M., editors. *Handbook of the Economics of Giving, Altruism and Reciprocity: Foundations*, 615–91.

Fiedler, S., Glöckner, A., Nicklisch, A., Dickert, S. (2013). Social value orientation and information search in social dilemmas: an eye-tracking analysis. *Organizational Behavior and Human Decision Processes*, **120**(2), 272–84.

Fischl, B., Sereno, M.I., Tootell, R.B., Dale, A.M. (1999). High-resolution intersubject averaging and a coordinate system for the cortical surface. *Human Brain Mapping*, **8**(4), 272–84.

Fischl, B., Dale, A.M. (2000). Measuring the thickness of the human cerebral cortex from magnetic resonance images. *Proceedings of the National Academy of Sciences of the United States of America*, **97**(20), 11050–5.

Freedman, D., Lane, D. (1983). A nonstochastic interpretation of reported significance levels. *Journal of Business and Economic Statistics*, **1**(4), 292–8.

Gallagher, H.L., Frith, C.D. (2003). Functional imaging of 'theory of mind'. *Trends in Cognitive Sciences*, **7**(2), 77–83.

Haas, B.W., Ishak, A., Anderson, I.W., Filkowski, M.M. (2015). The tendency to trust is reflected in human brain structure. *NeuroImage*, **107**, 175–81.

Hare, T.A., Camerer, C.F., Rangel, A. (2009). Self-control in decision-making involves modulation of the VMPFC valuation system. *Science*, **324**(5927), 646–8.

Haruno, M., Kimura, M., Frith, C.D. (2014). Activity in the nucleus accumbens and amygdala underlies individual differences in prosocial and individualistic economic choices. *Journal of Cognitive Neuroscience*, **26**(8), 1861–70.

Hung, J., Wang, X., Wang, X., Bi, Y. (2020). Functional subdivisions in the anterior temporal lobes: a large scale meta-analytic investigation. *Neuroscience and Biobehavioral Reviews*, **115**, 134–45.

Isik, L., Koldewyn, K., Beeler, D., Kanwisher, N. (2017). Perceiving social interactions in the posterior superior temporal sulcus. *Proceedings of the National Academy of Sciences of the United States of America*, **114**(43), E9145–52.

Kanagaretnam, K., Mestelman, S., Nainar, K., Shehata, M. (2009). The impact of social value orientation and risk attitudes on trust and reciprocity. *Journal of Economic Psychology*, **30**(3), 368–80.

Kennerley, S.W., Walton, M.E., Behrens, T.E., Buckley, M.J., Rushworth, M.F. (2006). Optimal decision making and the anterior cingulate cortex. *Nature Neuroscience*, **9**(7), 940–7.

Kerns, J.G., Cohen, J.D., MacDonald, A.W., Cho, R.Y., Stenger, V.A., Carter, C.S. (2004). Anterior cingulate conflict monitoring and adjustments in control. *Science*, **303**(5660), 1023–6.

Kitayama, S., Yanagisawa, K., Ito, A., Ueda, R., Uchida, Y., Abe, N. (2017). Reduced orbitofrontal cortical volume is associated with interdependent self-construal. *Proceedings of the National Academy of Sciences of the United States of America*, **114**(30), 7969–74.

Koechlin, E., Hyafil, A. (2007). Anterior prefrontal function and the limits of human decision-making. *Science*, **318**(5850), 594–8.

Kragel, P.A., Kano, M., Van Oudenhove, L., *et al*. (2018). Generalizable representations of pain, cognitive control, and negative emotion in medial frontal cortex. *Nature Neuroscience*, **21**(2), 283–9.

Lamm, C., Decety, J., Singer, T. (2011). Meta-analytic evidence for common and distinct neural networks associated with directly experienced pain and empathy for pain. *NeuroImage*, **54**(3), 2492–502.

Levy, D., Glimcher, P. (2012). The root of all value: a neural common currency for choice. *Current Opinion in Neurobiology*, **22**(6), 1027–38.

Lewis, P.A., Roozbeh, R., Brown, R., Roberts, N., Dunbar, R. (2011). Ventromedial prefrontal volume predicts understanding of others and social network size. *NeuroImage*, **57**(4), 1624–9.

Liebrand, W.B. (1984). The effect of social motives, communication and group size on behaviour in an N-person multi-stage mixed-motive game. *European Journal of Social Psychology*, **14**(3), 239–64.

Liebrand, W.B., McClintock, C.G. (1988). The ring measure of social values: a computerized procedure for assessing individual differences in information processing and social value orientation. *European Journal of Personality*, **2**(3), 217–30.

Liu, X., Hairston, J., Schrier, M., Fan, J. (2011). Common and distinct networks underlying reward valence and processing stages: a meta-analysis of functional neuroimaging studies. *Neuroscience and Biobehavioral Reviews*, **35**(5), 1219–36.

Liu, Y., Li, S., Lin, W., *et al*. (2019). Oxytocin modulates social value representations in the amygdala. *Nature Neuroscience*, **22**(4), 633–41.

Maguire, E.A., Gadian, D.G., Johnsrude, I.S., *et al*. (2000). Navigation-related structural change in the hippocampi of taxi drivers. *Proceedings of the National Academy of Sciences of the United States of America*, **97**(8), 4398–403.

McKenna, R., Rushe, T., Woodcock, K.A. (2017). Informing the structure of executive function in children: a meta-analysis of functional neuroimaging data. *Frontiers in Human Neuroscience*, **11**, 154.

Molenberghs, P., Cunnington, R., Mattingley, J.B. (2012). Brain regions with mirror properties: a meta-analysis of 125 human fMRI studies. *Neuroscience and Biobehavioral Reviews*, **36**(1), 341–9.

Molenberghs, P., Johnson, H., Henry, J.D., Mattingley, J.B. (2016). Understanding the minds of others: a neuroimaging meta-analysis. *Neuroscience and Biobehavioral Reviews*, **65**, 276–91.

Moll, J., de Oliveira-souza, R., Bramati, I.E. Grafman, J. (2002). Functional networks in emotional moral and nonmoral social judgments. *NeuroImage*, **16**(3), 696–703.

Morishima, Y., Schunk, D., Bruhin, A., Ruff, C.C., Fehr, E. (2012). Linking brain structure and activation in temporoparietal junction to explain the neurobiology of human altruism. *Neuron*, **75**(1), 73–9.

Muhlert, N., Lawrence, A.D. (2015). Brain structure correlates of emotion-based rash impulsivity. *NeuroImage*, **115**, 138–46.

Murphy, R.O., Ackerman, K.A. (2014). Social value orientation: theoretical and measurement issues in the study of social preferences. *Personality and Social Psychology Review*, **18**(1), 13–41.

Nash, K., Gianotti, L.R., Knoch, D. (2015). A neural trait approach to exploring individual differences in social preferences. *Frontiers in Behavioral Neuroscience*, **8**, 458.

Pan, J., Sawyer, K., McDonough, E.K., Slotpole, L., Gansler, D. (2018). Cognitive, neuroanatomical, and genetic predictors

of executive function in healthy children and adolescents. *Developmental Neuropsychology*, **43**(7), 535–50.

Pletzer, J.L., Balliet, D., Joireman, J., Kuhlman, D.M., Voelpel, S.C., Van Lange, P.A. (2018). Social value orientation, expectations, and cooperation in social dilemmas: a meta-analysis. *European Journal of Personality*, **32**(1), 62–83.

Quallo, M.M., Price, C.J., Ueno, K., *et al.* (2009). Gray and white matter changes associated with tool-use learning in macaque monkeys. *Proceedings of the National Academy of Sciences of the United States of America*, **106**(43), 18379–84.

Rand, D.G., Greene, J.D., Nowak, M.A. (2013). Spontaneous giving and calculated greed. *Nature*, **489**(7416), 427–30.

Riccelli, R., Toschi, N., Nigro, S., Terracciano, A., Passamonti, L. (2017). Surface-based morphometry reveals the neuroanatomical basis of the five-factor model of personality. *Social Cognitive and Affective Neuroscience*, **12**(4), 671–84.

Rolls, E.T., Grabenhorst, F. (2008). The orbitofrontal cortex and beyond: from affect to decision-making. *Progress in Neurobiology*, **86**(3), 216–44.

Sallet, J., Mars, R.B., Noonan, M.P., *et al.* (2011). Social network size affects neural circuits in macaques. *Science*, **334**(6056), 697–700.

Saxe, R., Kanwisher, N. (2003). People thinking about thinking people: the role of the temporo-parietal junction in 'theory of mind'. *Neuroimage*, **19**(4), 1835–42.

Schlaffke, L., Lissek, S., Lenz, M., *et al.* (2015). Shared and nonshared neural networks of cognitive and affective theory-of-mind: a neuroimaging study using cartoon picture stories. *Human Brain Mapping*, **36**(1), 29–39.

Schurz, M., Radua, J., Aichhorn, M., Richlan, F., Perner, J. (2014). Fractionating theory of mind: a meta-analysis of functional brain imaging studies. *Neuroscience and Biobehavioral Reviews*, **42**, 9–34.

Schurz, M., Tholen, M.G., Perner, J., Mars, R.B., Sallet, J. (2017). Specifying the brain anatomy underlying temporo-parietal junction activations for theory of mind: a review using probabilistic atlases from different imaging modalities. *Human Brain Mapping*, **38**(9), 4788–805.

Shackman, A.J., Salomons, T.V., Slagter, H.A., Fox, A.S., Winter, J.J., Davidson, R.J. (2011). The integration of negative affect, pain and cognitive control in the cingulate cortex. *Nature Reviews. Neuroscience*, **12**(3), 154.

Shamay-Tsoory, S.G., Aharon-Peretz, J., Perry, D. (2009). Two systems for empathy: a double dissociation between emotional and cognitive empathy in inferior frontal gyrus versus ventromedial prefrontal lesions. *Brain*, **132**(3), 617–27.

Spreng, R.N., Mar, R.A., Kim, A.S. (2009). The common neural basis of autobiographical memory, prospection, navigation, theory of mind, and the default mode: a quantitative meta-analysis. *Journal of Cognitive Neuroscience*, **21**(3), 489–510.

Sul, S., Tobler, P.N., Hein, G., Leiberg, S., Jung, D., Fehr, E., Kim, H. (2015). Spatial gradient in value representation along the medial prefrontal cortex reflects individual differences in prosociality. *Proceedings of the National Academy of Sciences of the United States of America*, **112**(25), 7851–76.

Sul, S., Güroğlu, B., Crone, E.A., Chang, L.J. (2017). Medial prefrontal cortical thinning mediates shifts in other-regarding preferences during adolescence. *Scientific Reports*, **7**, 8510.

Triki, Z., Levorato, E., McNeely, W., Marshal, J., Bshary, R. (2019). Population densities predict forebrain size variation in the cleaner fish Labroides dimidiatus. *Proceedings of the Royal Society B*, **286**(1915), 20192108.

Van Dijk, E., De Dreu, C.K.W. (2021). Experimental games and social decision-making. *Annual Review of Psychology*, **72**, 415–38.

Van Lange, P.A. (1999). The pursuit of joint outcomes and equality in outcomes: an integrative model of social value orientation. *Journal of Personality and Social Psychology*, **77**(2), 337–49.

Van Overwalle, F. (2009). Social cognition and the brain: a meta-analysis. *Human Brain Mapping*, **30**(3), 829–58.

Van Overwalle, F., Baetens, K. (2009). Understanding others' actions and goals by mirror and mentalizing systems: a meta-analysis. *NeuroImage*, **48**(3), 564–84.

Winkler, A.M., Ridgway, G.R., Webster, M.A., Smith, S.M., Nichols, T.E. (2014). Permutation inference for the general linear model. *NeuroImage*, **92**, 381–97.

Wittmann, M.K., Lockwood, P.L., Rushworth, M.F.S. (2018). Neural mechanisms of social cognition in primates. *Annual Review of Neuroscience*, **41**, 99–118.

Yamagishi, T., Takagishi, H., Fermin, A.D., Kanai, R., Li, Y., Matsumoto, Y. (2016). Cortical thickness of the dorsolateral prefrontal cortex predicts strategic choices in economic games. *Proceedings of the National Academy of Sciences of the United States of America*, **113**(20), 5582–7.

Zahn, R., Moll, J., Krueger, F., Huey, E.D., Garrido, G., Grafman, J. (2007). Social concepts are represented in the superior anterior temporal cortex. *Proceedings of the National Academy of Sciences of the United States of America*, **104**(15), 6430–5.

Appendix

Table A1. Regression coefficients of social preferences on cortical thickness of brain parcels (ID, per Figure 1 and Table 1), controlling for age, gender and average cortical thickness (standard error in parentheses)

Parcel ID	Left hemisphere			Right hemisphere		
	SVO	Ws	Wo	SVO	Ws	Wo
1	1.61 e-4 (0.0004)	−0.14 (0.12)	−0.01 (0.07)	−0.749 e-4 (0.0005)	0.25 (0.13)	0.05 (0.07)
2	−4.5 e-4 (0.0003)	−0.10 (0.10)	−0.10 (0.06)	−9.50 e-4† (0.0003)	0.04 (0.10)	−0.14† (0.05)
3	−6.23 e-4 (0.0003)	0.01 (0.09)	−0.10 (0.05)	−8.27 e-4† (0.0004)	−0.03 (0.11)	−0.15† (0.06)
4	1.77 e-4 (0.0005)	0.08 (0.14)	0.03 (0.08)	2.90 e-4 (0.0004)	−0.15 (0.12)	0.01 (0.07)
5	2.43 e-4 (0.0004)	−0.12 (0.10)	0.02 (0.06)	4.29 e-4 (0.0003)	−0.12 (0.10)	0.05 (0.05)
6	1.95 e-4 (0.0003)	0.0004 (0.10)	0.02 (0.05)	2.53 e-4 (0.0003)	−0.05 (0.09)	0.02 (0.05)
7	1.23 e-4 (0.0003)	−0.08 (0.09)	−0.01 (0.05)	−3.38 e-4 (0.0004)	0.0008 (0.11)	−0.06 (0.06)
8	−3.98 e-4 (0.0005)	0.18 (0.06)	−0.01 (0.09)	4.55 e-4 (0.0006)	0.19 (0.16)	0.15 (0.09)
9	3.10 e-4 (0.0003)	0.07 (0.09)	0.06 (0.05)	4.45 e-4 (0.0003)	0.02 (0.10)	0.09 (0.05)
10	0.41 e-4 (0.0002)	−0.01 (0.06)	0.01 (0.03)	3.60 e-4 (0.0002)	−0.04 (0.07)	0.05 (0.04)
11	0.51 e-4 (0.0003)	0.03 (0.08)	0.01 (0.05)	−0.199 e-4 (0.0003)	0.02 (0.08)	0.01 (0.04)
12	3.55 e-4 (0.0003)	0.05 (0.10)	0.05 (0.06)	−6.91 e-4 (0.0003)	0.12† (0.10)	−0.10 (0.06)
13	−2.68 e-4 (0.0003)	−0.04 (0.09)	−0.05 (0.05)	1.47 e-4 (0.0003)	0.02 (0.14)	0.02 (0.05)
14	5.10 e-4 (0.0004)	0.14 (0.12)	0.08 (0.07)	4.84 e-4 (0.0005)	0.02 (0.32)	0.05 (0.08)
15	−13.0 e-4 (0.001)	0.08 (0.34)	−0.14 (0.19)	3.11 e-4 (0.0011)	−0.51 (0.32)	−0.07 (0.18)
16	−1.87 e-4 (0.0003)	−0.02 (0.07)	−0.05 (0.04)	−3.40 e-4 (0.0002)	−0.05 (0.07)	−0.06 (0.04)
17	−3.66 e-4 (0.0005)	−0.01 (0.14)	−0.05 (0.08)	6.01 e-4 (0.0005)	−0.004 (0.15)	0.13 (0.08)
18	−3.08 e-4 (0.0002)	−0.04 (0.08)	−0.05 (0.04)	1.63 e-4 (0.0003)	−0.03 (0.08)	0.03 (0.04)
19	3.79 e-4 (0.0004)	−0.11 (0.10)	0.04 (0.06)	0.758 e-4 (0.0003)	0.04 (0.08)	0.02 (0.05)
20	−1.27 e-4 (0.0002)	−0.01 (0.06)	−0.01 (0.04)	3.30 e-4 (0.0002)	−0.01 (0.07)	0.06 (0.04)
21	1.94 e-4 (0.0007)	0.0014 (0.20)	0.02 (0.11)	−8.70 e-4 (0.0006)	0.23 (0.17)	−0.09 (0.10)
22	**1.69 e-4**** (0.0005)	−0.08 (0.15)	**0.26*** (0.08)	8.77 e-4† (0.0004)	−0.08 (0.12)	0.13 (0.07)
23	3.95 e-4 (0.0004)	0.08 (0.12)	0.07 (0.07)	−2.30 e-4 (0.0004)	0.03 (0.11)	−0.03 (0.06)
24	−5.33 e-4 (0.0008)	−0.24 (0.22)	−0.15 (0.12)	−1.28 e-4 (0.0007)	−0.17 (0.20)	−0.06 (0.11)
25	−2.71 e-4 (0.0003)	−0.09 (0.09)	−0.05 (0.05)	0.281 e-4 (0.0003)	0.01 (0.09)	0.02 (0.05)
26	1.37 e-4 (0.0003)	0.12 (0.09)	0.06 (0.05)	−0.240 e-4 (0.0003)	0.24† (0.09)	0.05 (0.05)
27	−12.8 e-4 (0.0008)	−0.26 (0.24)	−0.24 (0.14)	2.21 e-4 (0.0011)	−0.23 (0.31)	−0.03 (0.18)
28	1.82 e-4 (0.0003)	−0.03 (0.08)	0.02 (0.04)	3.39 e-4 (0.0003)	−0.05 (0.07)	0.05 (0.04)
29	70.4 e-4 (0.0003)	0.06 (0.09)	0.01 (0.05)	3.62 e-4 (0.0004)	−0.17 (0.11)	−0.004 (0.06)
30	−9.25 e-4 (0.0008)	0.13 (0.22)	−0.12 (0.13)	4.11 e-4 (0.0008)	0.20 (0.22)	0.13 (0.12)
31	1.86 e-4 (0.0006)	−0.03 (0.17)	−0.02 (0.10)	1.18 e-4 (0.0007)	0.08 (0.21)	0.16 (0.12)
32	2.18 e-4 (0.0005)	−0.01 (0.16)	0.02 (0.09)	3.46 e-4 (0.0005)	0.14 (0.14)	0.07 (0.08)
33	3.22 e-4 (0.0003)	−0.06 (0.09)	0.02 (0.05)	−1.67 e-4 (0.0003)	0.03 (0.08)	−0.04 (0.04)
34	−0.031 e-4 (0.0003)	−0.09 (0.08)	−0.03 (0.05)	1.22 e-4 (0.0003)	−0.10 (0.08)	−0.01 (0.05)
35	0.448 e-4 (0.0003)	0.04 (0.08)	0.01 (0.04)	−0.457 e-4 (0.0003)	0.005 (0.09)	0.0006 (0.05)
36	−1.69 e-4 (0.0003)	−0.05 (0.09)	−0.04 (0.05)	1.58 e-4 (0.0004)	−0.08 (0.10)	0.01 (0.06)
37	−4.56 e-4 (0.0003)	0.09 (0.08)	−0.07 (0.04)	−3.36 e-4 (0.0003)	−0.02 (0.07)	−0.06 (0.04)
38	5.17 e-4 (0.0003)	−0.01 (0.09)	0.06 (0.05)	−1.78 e-4 (0.0003)	0.06 (0.08)	−0.01 (0.04)
39	1.28 e-4 (0.0005)	−0.09 (0.13)	0.02 (0.07)	6.17 e-4 (0.0005)	−0.17 (0.14)	0.07 (0.08)
40	16.3 e-4† (0.0008)	−0.27 (0.23)	0.18 (0.13)	1.60 e-4 (0.0005)	0.06 (0.14)	0.05 (0.08)
41	0.785 e-4 (0.0002)	−0.01 (0.06)	0.01 (0.04)	−2.12 e-4 (0.0002)	0.03 (0.07)	−0.02 (0.04)
42	1.50 e-4 (0.0003)	0.10 (0.10)	0.04 (0.06)	−2.38 e-4 (0.0003)	0.12 (0.09)	−0.01 (0.05)
43	2.83 e-4 (0.0002)	−0.06 (0.06)	0.02 (0.04)	−2.47 e-4 (0.0003)	−0.06 (0.08)	−0.04 (0.04)
44	1.75 e-4 (0.0003)	0.05 (0.09)	0.04 (0.05)	−1.93 e-4 (0.0003)	0.11 (0.09)	−0.002 (0.05)
45	−4.09 e-4 (0.0005)	0.03 (0.15)	−0.06 (0.09)	−5.46 e-4 (0.0005)	−0.12 (0.14)	−0.11 (0.08)
46	−4.83 e-4 (0.0004)	−0.02 (0.11)	−0.07 (0.06)	1.23 e-4 (0.0004)	−0.11 (0.10)	0.001 (0.06)
47	9.07 e-4 (0.0007)	−0.10 (0.20)	0.14 (0.11)	11.8 e-4 (0.0006)	−0.23 (0.19)	0.13 (0.10)
48	−3.05 e-4 (0.0004)	0.03 (0.11)	−0.05 (0.06)	−6.21 e-4 (0.0004)	−0.14 (0.12)	−0.13 (0.07)
49	0.788 e-4 (0.0003)	−0.16 (0.10)	−0.01 (0.05)	2.39 e-4 (0.0003)	−0.10 (0.10)	0.02 (0.05)
50	0.353 e-4 (0.0003)	0.11 (0.09)	0.03 (0.05)	−0.582 e-4 (0.0003)	0.01 (0.10)	−0.01 (0.06)
51	3.52 e-4 (0.0007)	−0.17 (0.21)	0.01 (0.12)	2.66 e-4 (0.0005)	−0.15 (0.14)	0.03 (0.08)
52	−2.28 e-4 (0.0006)	−0.18 (0.18)	−0.06 (0.10)	−1.76 e-4 (0.0008)	0.18 (0.22)	0.02 (0.12)
53	3.47 e-4 (0.0003)	−0.05 (0.09)	0.06 (0.05)	4.29 e-4 (0.0003)	0.01 (0.08)	0.07 (0.05)
54	3.75 e-4 (0.0005)	0.08 (0.14)	0.10 (0.08)	2.07 e-4 (0.0005)	0.07 (0.14)	0.06 (0.08)
55	5.08 e-4 (0.0003)	−0.05 (0.08)	0.07 (0.05)	6.16 e-4† (0.0003)	0.03 (0.09)	0.09 (0.05)
56	6.34 e-4 (0.0006)	0.10 (0.17)	0.13 (0.10)	9.06 e-4 (0.0006)	0.10 (0.16)	0.17 (0.09)
57	−5.56 e-4 (0.0005)	0.07 (0.14)	−0.08 (0.08)	−11.4 e-4† (0.0005)	0.27 (0.15)	−0.13 (0.08)
58	−2.38 e-4 (0.0004)	0.09 (0.11)	0.01 (0.06)	4.92 e-4 (0.0004)	−0.30† (0.12)	0.05 (0.07)

(continued)

Table A1. (Continued)

Parcel ID	Left hemisphere			Right hemisphere		
	SVO	Ws	Wo	SVO	Ws	Wo
59	1.30 e-4 (0.0003)	−0.04 (0.09)	0.02 (0.05)	0.612 e-4 (0.0003)	−0.10 (0.10)	0.0004 (0.06)
60	3.34 e-4 (0.0003)	−0.10 (0.10)	0.05 (0.05)	4.54 e-4 (0.0004)	0.11 (0.10)	0.11 (0.06)
61	−1.15 e-4 (0.0002)	0.06 (0.06)	0.01 (0.03)	−0.854 e-4 (0.0002)	−0.02 (0.06)	−0.02 (0.03)
62	−8.47 e-4 (0.0007)	0.27 (0.19)	−0.08 (0.11)	5.76 e-4 (0.0006)	−0.20 (0.17)	0.05 (0.10)
63	−5.69 e-4 (0.0003)	−0.13 (0.10)	−0.12† (0.06)	−2.56 e-4 (0.0004)	−0.05 (0.11)	−0.04 (0.06)
64	−3.09 e-4 (0.0003)	−0.17 (0.10)	−0.08 (0.06)	−4.71 e-4 (0.0003)	0.20† (0.09)	−0.04 (0.05)
65	−2.24 e-4 (0.0003)	0.07 (0.08)	−0.03 (0.05)	−3.84 e-4 (0.0003)	0.04 (0.07)	−0.05 (0.04)
66	−1.73 e-4 (0.0004)	0.02 (0.11)	−0.03 (0.06)	−3.59 e-4 (0.0004)	0.003 (0.10)	−0.07 (0.06)
67	1.74 e-4 (0.0003)	−0.03 (0.09)	0.02 (0.05)	2.93 e-4 (0.0003)	0.09 (0.09)	0.07 (0.05)
68	1.23 e-4 (0.0003)	−0.01 (0.09)	0.02 (0.05)	0.360 e-4 (0.0003)	−0.13 (0.09)	−0.02 (0.05)
69	8.93 e-4 (0.0006)	−0.04 (0.17)	0.14 (0.10)	−2.56 e-4 (0.0006)	−0.11 (0.17)	−0.07 (0.09)
70	−6.58 e-4 (0.0004)	0.01 (0.10)	−0.11 (0.06)	−2.90 e-4 (0.0003)	−0.05 (0.08)	−0.07 (0.05)
71	2.77 e-4 (0.0003)	0.07 (0.10)	0.07 (0.05)	2.89 e-4 (0.0003)	−0.10 (0.10)	0.01 (0.06)
72	−2.77 e-4 (0.0003)	0.16 (0.10)	−0.01 (0.05)	−2.28 e-4 (0.0004)	0.22 (0.11)	0.02 (0.06)
73	−3.53 e-4 (0.0003)	0.14 (0.09)	0.00 (0.05)	−3.21 e-4 (0.0003)	−0.02 (0.09)	−0.06 (0.05)
74	2.64 e-4 (0.0004)	−0.08 (0.11)	0.03 (0.06)	−1.18 e-4 (0.0004)	−0.03 (0.10)	−0.01 (0.06)

SVO = social value orientation degree; Ws = Weight to Self; Wo = Weight to Other. †$p < 0.05$ before permutations;
**$p < 0.01$ after permutations;
*$p < 0.1$ after permutations.